

# Emergent Universe Scenario in the Modified Chaplygin gas : Towards an Exact Solution and Observational Constraints

D. Panigrahi\*, S. Chatterjee †, B. C. Paul‡

## Abstract

The Modified Chaplygin Gas (MCG) model has been revisited to explore its capability of reproducing the entire cosmic evolution within a single theoretical framework. The field equation is highly nonlinear which does not permit an explicit analytical solution in a simple functional form of cosmic time. The evolution of cosmological quantities—such as the scale factor, the flip time, and other dynamical parameters cannot be described in a known functional form. To overcome the limitation and to determine the flip time along with other physical characteristics of the cosmological model, we adopt an *alternative approach* here. By employing a first-order approximation, we derive an exact analytical expression for the scale factor, which determines the flip time. Remarkably, it is noted that the program adopted here yields an emergent-type, non-singular cosmological solution assuming the first-order binomial approximation. In this scenario, the universe begins with a finite minimum size ( $a_{\min}$ ) which undergoes a smooth transition from a quasi-static phase to an exponential de Sitter-like expansion at late times, admitting a phase of expansion with  $\Lambda$ CDM limit. The equation of state parameters ( $\alpha$  and  $A$ ) are constrained using the observed Hubble Data, and for a physical viable cosmology we estimate a acceptable range of values:  $0 < \alpha < 1$ ,  $0 < A < 1/3$ . The effective equation-of-state parameter  $w_{\text{eff}}$  is found to evolve from a positive value in the early matter-dominated era to  $w_{\text{eff}} \approx -1$  in the late time universe, which is consistent with the current observations. Furthermore, the Raychaudhuri-based reinterpretation leads to excellent agreement with the statistical constraints, reinforcing the robustness of the methodology. Overall, the study establishes that MCG is self-consistent and accommodates late-time cosmic acceleration without invoking any modification in general relativity.

KEY WORDS : cosmology; accelerating universe; chaplygin gas

PACS : 04.20, 04.50 +h

## 1 Introduction

Following the discovery of high-redshift Type Ia supernovae [1], it became evident that within the framework of the standard Friedmann–Robertson–Walker (FRW) cosmology—assuming homogeneity

\*Netaji Nagar Day College, 170/436 N.S. C. Bose Road, Regent Estate, Kolkata 700092, INDIA and also Relativity and Cosmology Research Centre, Jadavpur University, Kolkata - 70032, India , e-mail: dubyendupanigrahi@yahoo.co.in, dpanigrahi@nndc.ac.in

†New Alipore College (Retd.), Kolkata - 700053, India and also Relativity and Cosmology Research Centre, Jadavpur University, Kolkata - 700032, India, e-mail : chat\_sujit1@yahoo.com

‡Department of Physics, University of North Bengal, Dist.-Darjeeling, PIN-734013, India, e-mail : bc-paul@associates.iucaa.in

and isotropy —the universe is presently undergoing an accelerated phase of expansion. Observations indicate that baryonic matter contributes only about four percent of the total energy density, while the remaining components are of non-baryonic type. Independent evidence from Cosmic Microwave Background Radiation (CMBR) measurements [2] also supports this accelerated expansion, thereby motivating extensive theoretical and observational efforts to understand its origin.

The fundamental challenge lies in identifying the mechanism responsible for this late-time acceleration. Broadly, two main theoretical approaches have been proposed to address the late acceleration: (i) modifications of Einstein’s general theory of relativity, and (ii) the introduction of a new cosmic fluid—often identifying an evolving cosmological constant or a dynamical scalar field such as quintessence. However, both the approaches face significant theoretical and conceptual issues. The phenomenon is generally attributed to an exotic component of the cosmic fluid, known as *dark energy* (DE), which accounts for nearly three-fourths of the total energy density of the universe. Another crucial yet equally elusive component is *dark matter* (DM), which provides the necessary gravitational pull to explain galaxy formation and large-scale structure.

Despite numerous attempts, identifying the true nature of DE for the first case remains one of the most profound unresolved problem in cosmology. Over the past few decades, a wide range of DE models have been explored, including quintessence [3], phantom fields [4], holographic dark energy [5], string-inspired models [6], Born–Infeld condensates [7], modified gravity theories [8], and inhomogeneous cosmological scenarios [9]. Comprehensive reviews of these models are available in the literature [10].

Although the evolving cosmological constant ( $\Lambda$ ) provides a simplest explanation for the observed acceleration in the second case, it suffers from two major theoretical challenges: (i) the *fine-tuning problem*, since the observed value of  $\Lambda$  is vastly smaller than that predicted by quantum field theory, and (ii) the *cosmic coincidence problem*, arising from the near equality of the present-day matter and vacuum energy densities despite their different evolutionary histories. While the  $\Lambda$ CDM model remains consistent with observations, these issues diminish its theoretical appeal. Attempts to generalize  $\Lambda$  to a variable form introduces further complications [11, 12], while alternative frameworks such as brane-world cosmology [13, 14, 15] is also considered to invoke extra spatial dimensions that remain speculative.

However, among the alternative approaches, the *Chaplygin Gas* (CG) model has emerged as an intriguing candidate. It is characterized by the equation of state (EoS)

$$p = -\frac{B}{\rho}, \quad (1)$$

where  $\rho$  and  $p$  denote the energy density and pressure, respectively, and  $B$  is a positive constant [16]. Although the CG model successfully explains supernova data, it fails to reproduce the observed structure formation and exhibits unphysical oscillations in the matter power spectrum [17]. Thus CG is generalized, assuming a *Generalized Chaplygin Gas* (GCG) which is

$$p = -\frac{B}{\rho^\alpha}, \quad (2)$$

where  $0 < \alpha < 1$  [18]. The GCG model can effectively reproduce the background dynamics of a homogeneous and isotropic universe and mimic the  $\Lambda$ CDM model at late times. However, it suffers from strong oscillations or instabilities in the matter power spectrum unless it effectively reduces to  $\Lambda$ CDM [19]. A further refinement in the EoS named, the *Modified Chaplygin Gas* (MCG) model [20, 21] was proposed. MCG introduces an additional term linear in  $\rho$ , leading to an EoS of two different

parameters ( $\alpha$  and  $A$ ),

$$p = A\rho - \frac{B}{\rho^\alpha}. \quad (3)$$

The MCG model provides a unified description of dark matter and dark energy within a single fluid framework. It exhibits a radiation-dominated behavior at high densities (for  $A = \frac{1}{3}$ ), transitions through a matter-dominated phase, and asymptotically approaches a cosmological constant-like behavior at low densities. Thus, a universe filled with MCG consistently evolves from radiation epoch to the present dark energy-dominated phase, finally entering into the  $\Lambda$ CDM limiting case. A number of studies in the literature revealed various aspects of the MCG model, Wu *et al.* [22] explored its dynamical properties, Bedran *et al.* [23] examined the temperature evolution in its presence, and later works demonstrated its consistency with perturbative analyses [24] and spherical collapse scenarios [25] where Febris et al studied and ruled out the constant  $A$ . In the present work, we revisit a spatially flat Friedmann–Robertson–Walker (FRW) universe filled with a Modified Chaplygin Gas (MCG) and perform a detailed cosmological analysis to constrain its model parameters making use of observations. Using the standard  $\chi^2$ -minimization technique, we determine the best-fit values of the MCG parameters from the Hubble–57 dataset and employ these results to investigate the dynamical evolution of the universe.

It is important to note that the key Eq. (10) does not admit an explicit analytic solution for the scale factor with a known functional form. Consequently, the time evolution of several cosmological quantities—such as evolution of the scale factor, the flip time etc. — cannot be obtained in closed form. To overcome this limitation in order to explore the temporal behavior of these quantities, we adopt an alternative analytical approach that enables us to study the underlying dynamics more transparently. Furthermore, the concept of an emergent universe—a cosmological scenario where the universe is eternally existing and originates from a quasi-static state before entering an inflationary expansion—has been widely investigated in recent years [26, 27, 28]. Such model, consistent with the classical Lemaître–Eddington framework, offer an elegant resolution to the initial singularity problem inherent in the standard Big Bang cosmology. A physically consistent emergent universe model naturally addresses several conceptual issues of the Big Bang scenario. For instance, Mukherjee *et al.* [29] obtained an emergent-type solution by setting a negative  $\alpha$  ( $\alpha = -\frac{1}{2}$ ) in Eq. (3), whereas Dutta *et al.* [30] claimed that such non-singular model is not possible within the conventional MCG framework. In the paper, we demonstrated that the analysis—based on Eq. (54)—reveals a new class of emergent-type cosmology that arises from the MCG equation of state under the first order approximation with the following conditions  $0 < A < \frac{1}{3}$  and  $0 < \alpha < 1$ .

The paper is organized as follows. In Sec. 2, we present the fundamental field equations derived from Einstein’s equations. Sec. 3 is devoted to the mathematical formulation of the model, which leads to a hypergeometric-type solution. In this section, we also derive the expressions for the deceleration parameter, the effective equation of state, and the redshift corresponding to the transition (flip) time. It is shown that the model asymptotically approaches the  $\Lambda$ CDM behavior at late cosmic times, and its dynamical evolution is illustrated graphically. In Sec. 4, we highlight a noteworthy aspect of our analysis, where a first-order approximation of the key dynamical equation is considered. This approximation allows for an exact analytical expression of the scale factor to be obtained. A detailed investigation of the flip time is carried out both analytically and graphically. In Sec. 5, we show that the model admits an emergent universe scenario in the phantom regime for integration constant  $c < 0$ . The evolution of the scale factor, the effective equation of state, the deceleration parameter, and the energy density are analyzed comprehensively. Furthermore, the model parameters are constrained using the Hubble 57 data points through a standard  $\chi^2$ -minimization technique. Sec. 6 discusses the

physical implications of the results within the framework of the Raychaudhuri equation. Finally, Sec. 7 summarizes the main findings and presents the concluding remarks.

## 2 Field Equations

We consider a spherically symmetric homogeneous spacetime given by

$$ds^2 = dt^2 - a^2(t) \{dr^2 + r^2 (d\theta^2 + \sin^2 \theta d\phi^2)\} \quad (4)$$

where the scale factor,  $a(t)$  depends on time only.

The energy momentum tensor is given by

$$T_\nu^\mu = (\rho + p)\delta_0^\mu\delta_\nu^0 - p\delta_\nu^\mu \quad (5)$$

where  $\rho(t)$  is the matter density and  $p(t)$  the isotropic pressure. Here we consider a comoving coordinate system such that  $u^0 = 1, u^i = 0$  ( $i = 1, 2, 3$ ) and  $g^{\mu\nu}u_\mu u_\nu = 1$  where  $u_i$  is the 4- velocity.

The independent field equations for the metric Eq. (4) and the energy momentum tensor Eq. (5) are given by

$$3\frac{\dot{a}^2}{a^2} = 3H^2 = \rho \quad (6)$$

$$2\frac{\ddot{a}}{a} + \frac{\dot{a}^2}{a^2} = 2(\dot{H} + H) = -p \quad (7)$$

where  $H$  is the Hubble parameter. Now from the conservation law for homogeneous model

$$\dot{\rho} + 3H(\rho + p) = 0 \quad (8)$$

At this stage, we assume that the cosmic fluid is governed by the Modified Chaplygin Gas (MCG) equation of state, as given in Eq. (3). Using Eqs (3) & (8) and performing straightforward algebraic manipulations, we obtain the following expression for the energy density

$$\rho = \left[ \frac{B}{(1+A)} + c(1+z)^{3(1+\alpha)(1+A)} \right]^{\frac{1}{1+\alpha}} \quad (9)$$

where  $c$  is an integration constant. Plugging in the expression of  $\rho$  from Eqs (6) and (9) we finally get

$$3\frac{\dot{a}^2}{a^2} = 3H^2 = \left[ \frac{B}{(1+A)} + c(1+z)^{3(1+\alpha)(1+A)} \right]^{\frac{1}{1+\alpha}} \quad (10)$$

## 3 Cosmological dynamics

The dynamics of the MCG model in a 4D framework have been studied extensively [20, 21], with perturbative analyses highlighting several generic features [24]. Notably, Fabris *et al.* [25] used perturbative methods to compare the model with observational data, concluding from power spectrum analyses that  $A < 10^{-6}$ , effectively reducing the model to the GCG and almost ruling out the MCG.

Furthermore, recent supernova data suggest that negative values of  $\alpha$  are favored [31], though such values may imply imaginary sound speeds and potential instabilities [32, 33, 34]. Conversely, it has been argued that  $\alpha > 1$  is also possible [35], though such cases risk superluminal sound speeds.

### 3.1 Square speed of sound:

The adiabatic sound speed squared in the Modified Chaplygin Gas (MCG) model, defined by the Eq. (3) is given by

$$c_s^2 = \frac{\partial p}{\partial \rho} = A + \alpha \frac{B}{\rho^{\alpha+1}} \quad (11)$$

For physical viability, the sound speed must remain real, positive, and subluminal, i.e.,  $0 \leq c_s^2 \leq 1$ .

- (i) Early Universe ( $\rho \gg 1$ ): In the high-density regime, the second term in the equation of state is negligible, so the effective sound speed approaches  $c_s^2 \rightarrow A$ . Thus, the parameter  $A$  governs the early-time behavior of the fluid. To mimic radiation- or dust-like matter, one typically requires  $0 \leq A \leq \frac{1}{3}$ , which ensures consistency with nucleosynthesis and structure formation.
- (ii) Late Universe ( $\rho \ll 1$ ): As the density decreases with cosmic expansion, the second term grows, and  $c_s^2 \simeq \alpha \frac{B}{\rho^{\alpha+1}}$ . This can diverge and exceed unity unless  $\alpha$  is sufficiently small. Rearranging the causality condition yields  $\alpha \leq \frac{(1-A)\rho^{\alpha+1}}{B}$ . Hence, the upper bound on  $\alpha$  is density-dependent and becomes increasingly restrictive as  $\rho \rightarrow 0$ . This feature reflects the MCG's transition from matter-like to dark-energy-dominated behavior, with the equation of state naturally softening at low densities.

To ensure stability and consistency with cosmology, the following parameter ranges are commonly imposed:  $0 \leq A \leq \frac{1}{3}$ ,  $0 \leq \alpha < 1$ ,  $B > 0$ . These conditions guarantee that the sound speed remains real, subluminal, and stable under perturbations throughout cosmic evolution. In our analysis, we have consistently imposed and maintained these allowed parameter ranges.

An exact closed-form solution for the scale factor  $a(t)$  from Eq. (10) is difficult to obtain, as the integration results in an elliptic form. However, the equation yields valuable information in certain limiting cases as discussed below.

### 3.2 Deceleration Parameter:

During the early phase of cosmological evolution, with a relatively small scale factor  $a(t)$ , the second term in Eq. (10) becomes dominant. This regime has already been addressed in detail in the literature [20, 21], so we only summarize the main point here. From the expression of the deceleration parameter  $q$ , it follows that

$$q = -\frac{1}{H^2} \frac{\ddot{a}}{a} = \frac{d}{dt} (H^{-1}) - 1 = \frac{1}{2} + \frac{3}{2} \frac{p}{\rho} = \frac{1+3A}{2} - \frac{3B}{2} \frac{1}{\rho^{\alpha+1}} \quad (12)$$

which, by Eq. (9), gives

$$q = \frac{1+3A}{2} - \frac{3B}{2} \left[ \frac{B}{1+A} + C(1+z)^{3(1+\alpha)(1+A)} \right]^{-1} \quad (13)$$

To constrain the parameters, we consider  $\Omega_m = \frac{c}{\rho_0^{1+\alpha}}$  and  $\frac{B}{\rho_0^{1+\alpha}} = \rho_0^{1+\alpha}(1 - \Omega_m)$  and we can express the Eq. (13) as

$$q = \frac{1+3A}{2} - \frac{3}{2}(1+A)\frac{1-\Omega_m}{\Omega_m} \left[ \frac{1-\Omega_m}{\Omega_m} + (1+z)^{3(1+\alpha)(1+A)} \right]^{-1} \quad (14)$$

At the flip time  $q = 0$ , the redshift parameter at the flip time  $z_f$  [36, 37] is given by from Eq. (13) as

$$z_f = \left[ \frac{2B}{C} \frac{1}{(1+A)(1+3A)} \right]^{\frac{1}{3(1+\alpha)(1+A)}} - 1 \quad (15)$$

and from Eq. (14), we get

$$z_f = \left[ \frac{1-\Omega_m}{\Omega_m} \frac{2}{1+3A} \right]^{\frac{1}{3(1+A)(1+\alpha)}} - 1 \quad (16)$$

where  $z_f$  signifies the sign change of the deceleration parameter. For the universe to be accelerating at the present epoch (i.e., at  $z = 0$ ), we require  $z_f > 0$ , which gives from Eq. (13) as (i)  $B > \frac{c}{2}(1+3A)(1+A)$  and from Eqn. (14) as (ii)  $\Omega_m < \frac{2}{3(1+A)}$ , since  $0 \leq A \leq \frac{1}{3}$ , this is consistent with the current observational constraint on  $\Omega_m$ .

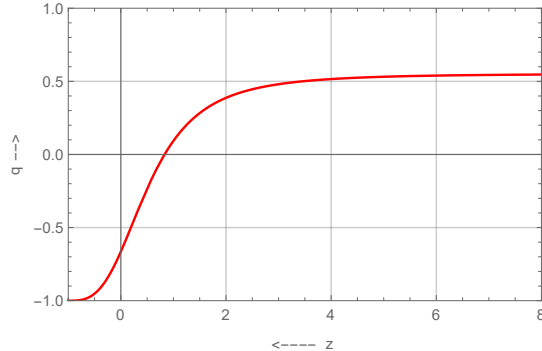


Figure 1: The variations of  $q$  and  $z$ .

As the universe expands, the energy density  $\rho$  decreases with time, causing the second term in Eq. (12) to increase. This indicates the occurrence of a transition (flip) when the density reaches a critical value  $\rho = \rho_{flip} = \left( \frac{3B}{1+3A} \right)^{\frac{1}{1+\alpha}}$ . Since  $A > 0$  and  $\alpha > 0$  correspond to a lower density at the transition epoch, they favor a later onset of cosmic acceleration. This indicates that the universe remains in the decelerating phase for an extended period before the dark-energy-like behavior of the Modified Chaplygin Gas drives acceleration.

The behavior of the deceleration parameter  $q$  at different epochs of cosmic evolution can be summarized as follows.

(i) At the early stage, when the redshift  $z$  is very high the Eq. (14) reduces to

$$q = \frac{1+3A}{2} \quad (17)$$

For the FRW model, during the radiation-dominated era,  $q = 1$ , which from Eq. (17) yields  $A = \frac{1}{3}$ .

(ii) At present epoch ( $z = 0$ ), the Eq. (14) reduces to

$$q = \frac{1+3A}{2} - \frac{3}{2}(1+A)(1-\Omega_m) \quad (18)$$

Since  $\Omega_m < \frac{2}{3(1+A)}$ , we obtain  $q < 0$ , which corresponds to an accelerating universe.

(iii) At the late stage of cosmic evolution, Eq. (14) reduces to  $q = -1$ , representing  $\Lambda$ CDM.

By setting  $A = 0$ , the present model reduces to the Generalized Chaplygin Gas (GCG) form. In this limit, the resulting expressions are identical to those reported in our earlier work [38].

Fig-1 illustrates the variation of the deceleration parameter  $q$  with redshift  $z$  in the framework of the Modified Chaplygin Gas (MCG) model. The universe transits from early deceleration ( $q > 0$ ) to late-time acceleration ( $q < 0$ ) at the flip redshift  $z_f$ , showing a smooth evolution without separate dark matter or dark energy components for dark matter and dark energy.

### 3.3 Effective equation of state:

From Eqs. (3) and (9), the effective equation of state parameter  $w_{\text{eff}}$  is obtained as

$$w_{\text{eff}} = \frac{p}{\rho} = A - \frac{B}{\rho^{1+\alpha}} = A - \frac{(1+A)(1-\Omega_m)}{1-\Omega_m + \Omega_m(1+z)^{3(1+A)(1+\alpha)}} \quad (19)$$

The effective equation of state parameter  $w_{\text{eff}}$  exhibits distinct behavior across different cosmic epochs as follows:

- (i) **Early Universe:** In the high-redshift limit, using Eq. (19), we find  $w_{\text{eff}} = A$ , corresponding to a radiation-dominated phase of the universe.
- (ii) **Dust dominated Epoch:** At the dust-dominated epoch, the effective equation-of-state parameter becomes  $w_{\text{eff}} = 0$ , which yields

$$z_{\text{dust}} = \left( \frac{1-\Omega_m}{A\Omega_m} \right)^{\frac{1}{3(1+A)(1+\alpha)}} - 1. \quad (20)$$

A comparison with the redshift at the flip time,  $z_f$ , shows that  $z_{\text{dust}} > z_f$ , implying that the onset of acceleration occurs after the dust-dominated era, which is consistent with the standard cosmological timeline of the evolution of the universe.

(iii) **Present Epoch:** In the present epoch ( $z = 0$ ), Eq. (19) simplifies to

$$w_{\text{eff}} = -1 + \Omega_m(1+A). \quad (21)$$

Since the maximum value of  $\Omega_m$  is  $(\Omega_m)_{\text{max}} = \frac{2}{3(1+A)}$ , this yields  $w_{\text{eff}} = -\frac{1}{3}$ . Therefore, at  $z = 0$ , we obtain  $-1 < w_{\text{eff}} < 0$ , which corresponds to an accelerating universe.

(iv) **Late Universe:** At the late stage of cosmic evolution, the Eq. (19) reduces to  $w_{\text{eff}} = -1$ , indicating that the model asymptotically approaches a state similar to a cosmological constant, effectively representing the scenario  $\Lambda$ CDM.

Thus, the model smoothly interpolates between a radiation-like early phase and a cosmological constant-like late phase, providing a consistent description of cosmic evolution.

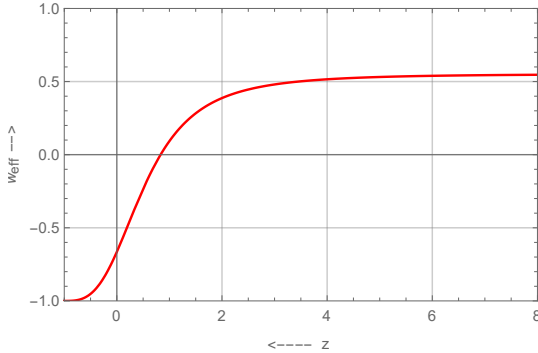


Figure 2: The variations of  $w_{\text{eff}}$  and  $z$ .

It may be noted that on setting  $A = 0$ , the effective equation of state reduces to that of the Generalized Chaplygin Gas (GCG) model, for which the derived expressions are consistent with those obtained in our earlier work [38].

Fig. 2 illustrates the evolution of the effective equation of state parameter  $w_{\text{eff}}$  with redshift  $z$  in the Modified Chaplygin Gas (MCG) model. At high redshift,  $w_{\text{eff}} > 0$  corresponds to a decelerated, matter-dominated phase, whereas near the present epoch,  $0 > w_{\text{eff}} > -1$  indicates an accelerated, dark energy-dominated expansion. At late times,  $w_{\text{eff}} \rightarrow -1$ , asymptotically approaching the  $\Lambda$ CDM limit. This behavior clearly demonstrates the smooth transition of the MCG model from an early decelerating phase to a late-time accelerated expansion.

### 3.4 Observational Constraints on the Model Parameters:

In this section, the Hubble-57 data [8] will be utilized to analyze the cosmological model by estimating the constraints imposed on the model parameters. Using the present value of the scale factor normalized to unity, *i.e.*,  $a = a_0 = 1$ , we obtain a relation between the Hubble parameter and the redshift parameter  $z$ . If  $\rho_0$  denotes the density at the present epoch, then the well-known density parameter is written as  $\Omega_m = \frac{c}{\rho_0^{1+\alpha}}$  [39]. Now, using Eq. (9), we can express the three-dimensional spatial matter density as

$$\rho = \rho_0 \left\{ 1 - \Omega_m + \Omega_m (1+z)^{3(1+A)(1+\alpha)} \right\}^{\frac{1}{1+\alpha}} \quad (22)$$

The Fig.-3 illustrates the evolution of the universe's density as a function of redshift,  $z$ . It shows that the matter density decreases as  $z$  decreases, consistent with expectations from cosmological models where matter dilutes as the universe expands. Now the Hubble parameter

$$H(z) = H_0 \left\{ 1 - \Omega_m + \Omega_m (1+z)^{3(1+A)(1+\alpha)} \right\}^{\frac{1}{2(1+\alpha)}} \quad (23)$$

where  $H_0 = \left(\frac{\rho_0}{3}\right)^{\frac{1}{2}}$  represents the present value of the Hubble parameter. The Eq. (23) describes the evolution of the Hubble parameter  $H(z)$  as a function of the redshift parameter  $z$ . In Fig.-4(a),

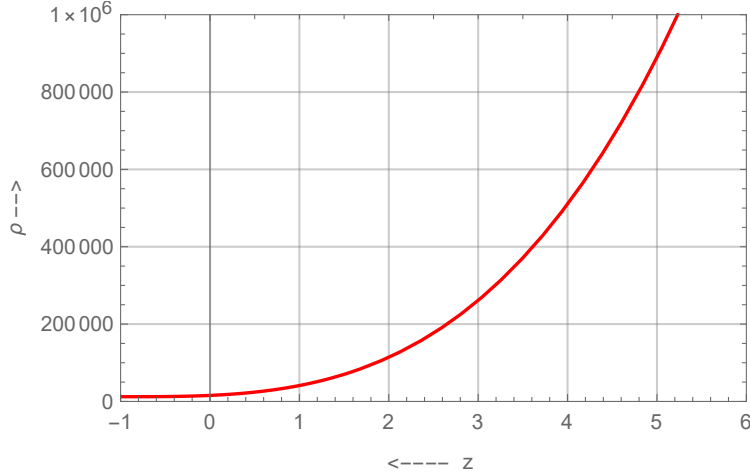


Figure 3: The variation of  $\rho$  with  $z$  is shown in this figure.

we present a best-fit curve of the redshift  $z$  against the Hubble parameter  $H(z)$  using the Hubble-57 data points. Furthermore, in Fig.-4(b), we compare the best-fit graph with the graph obtained from Eq. (23). These two graphs nearly coincide throughout the evolution, indicating that the behavior of our model is in good agreement with the observational data.

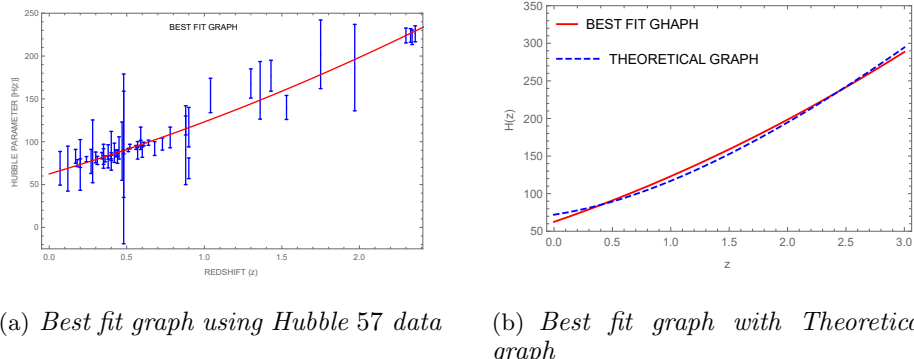


Figure 4:  $H(z)$  vs  $z$

The apparently small uncertainty of the measurement naturally increases its weightage in estimating  $\chi^2$  statistics. We define here the  $\chi^2$  as

$$\chi_H^2 = \sum_{i=1}^{30} \frac{[H^{\text{obs}}(z_i) - H^{\text{th}}(z_i, H_0, \theta)]^2}{\sigma_H^2(z_i)} \quad (24)$$

Here,  $H^{\text{obs}}$  represents the observed Hubble parameter at  $z_i$ , and  $H^{\text{th}}$  is the corresponding theoretical Hubble parameter given by Eq. (23). Additionally,  $\sigma_H(z_i)$  denotes the uncertainty for the  $i$ -th data point in the sample, and  $\theta$  represents the model parameter. In this work, we utilize the observational  $H(z)$  dataset, which consists of 57 data points spanning the redshift range  $0.07 \leq z \leq 2.36$  [38], extending beyond the redshift range covered by type Ia supernova observations. It is important to

note that the confidence levels  $1\sigma$  (68.3%),  $2\sigma$  (95.4%), and  $3\sigma$  (99.7%) correspond to  $\Delta\chi^2$  values of 2.3, 6.17, and 11.8, respectively, where  $\Delta\chi^2 = \chi^2(\theta) - \chi^2(\theta^*)$  and  $\chi_m^2$  is the minimum value of  $\chi^2$ . An important quantity used in the data fitting process is

$$\overline{\chi^2} = \frac{\chi_m^2}{dof} \quad (25)$$

where, the subscript  $dof$  represents the degrees of freedom, defined as the difference between the total number of observational data points and the number of free parameters. If  $\frac{\chi_m^2}{dof} \leq 1$ , it indicates a good fit, implying that the observed data are consistent with the considered model.

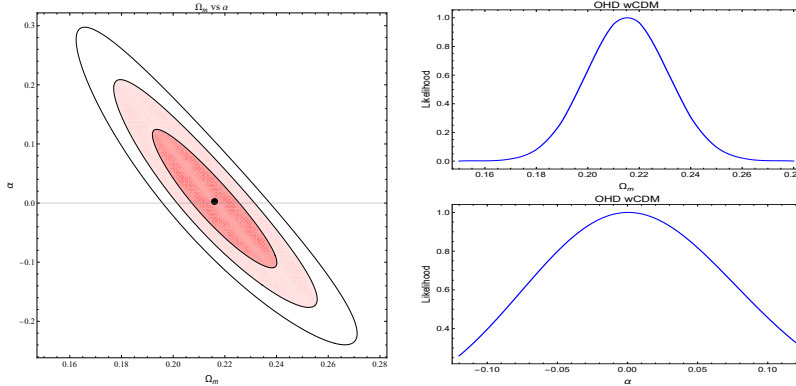


Figure 5:  $\Omega_m$  vs  $\alpha$  graph with likelihood

From the contour plot shown in Fig. 5, the values of the parameters  $\alpha$  and  $\Omega_m$  are determined for  $H_0 = 72 \text{ km s}^{-1} \text{ Mpc}^{-1}$  [40] and  $A = 0.034$ . The corresponding  $1\sigma$  confidence intervals, obtained using the Hubble dataset, are summarized in Table 1. The Modified Chaplygin Gas (MCG) model has been extensively investigated in the literature, and several studies have constrained its parameters using diverse observational datasets. For instance, L. Xu *et al.* [41] reported  $\alpha = 0.000727^{+0.00142+0.00393}_{-0.00140-0.00234}$  and  $A = 0.000777^{+0.000201+0.000915}_{-0.000302-0.000234}$  for  $H_0 = 72.561^{+1.679+3.361}_{-1.690-3.223}$ , which are comparatively smaller than the values obtained in the present analysis. Similarly, H. Li *et al.* [42] derived parameter constraints from various data combinations; for example, using CMB+CC data they found  $\alpha = -0.1688^{+0.1456+0.3340}_{-0.2143-0.3080}$  with  $H_0 = 65.75^{+2.60+6.18}_{-3.71-5.13}$ , whereas the combination CMB+JLA+CC yielded  $\alpha = 0.0181^{+0.1029+0.3953}_{-0.2199-0.3060}$  with  $H_0 = 68.07^{+2.72+5.30}_{-3.10-5.22}$ . On the other hand, J. Lu *et al.* [43] obtained  $\alpha = 1.724$  and  $A = -0.085$ , which are not physically viable within the MCG framework, since maintaining a subluminal sound speed requires  $0 < \alpha < 1$  and  $0 < A < \frac{1}{3}$ . As pointed out earlier, Fabris *et al.* [25] ruled out the case of constant  $A$ , while Lima *et al.* [44] showed that a small value of  $A$  is still admissible for  $0.9 < \alpha < 1$ .

Overall, although some discrepancies arise due to differences in datasets, priors, and statistical techniques, the general agreement among these studies underscores the robustness of the MCG model in describing the late-time accelerated expansion of the universe.

Table 1: Best-fit values of the  $\Omega_m$  and  $\alpha$  using Hubble-57 data ( $1\sigma$  confidence region).

Parameter	$H_0$ ( $\text{km s}^{-1} \text{ Mpc}^{-1}$ )	$A$	$\chi_m^2$	$\Omega_m$	$\alpha$
Best-fit values	72	0.034	46.48	0.216	0.0026
Range ( $1\sigma$ region)	—	—	—	0.1920, 0.2401	-0.1095, 0.1246

We consider only positive values of  $\alpha$  and  $A$ , as these parameters play crucial roles in defining the equation of state within the framework of the Modified Chaplygin Gas (MCG) model. Our analysis reveals that  $\alpha$  assumes small positive values satisfying  $0 < \alpha < 1$ , consistent with previous results [38]. Similarly, we adopt small positive values of  $A$ , which favor the existence of the MCG model—contrary to the conclusions of Fabris et al. [25], who ruled out its viability. These parameter choices are well supported by current observational constraints, which strongly favor small positive values of both  $\alpha$  and  $A$  to ensure compatibility with cosmological data.

It is noteworthy that this restriction differs significantly from the pure Chaplygin Gas model, characterized by  $\alpha = 1$  and  $A = 0$ . In contrast, the MCG model with  $0 < \alpha < 1$  and  $0 < A < \frac{1}{3}$  provides greater flexibility, enabling a smooth and realistic transition from a radiation-dominated era to a dark energy-dominated phase, thereby offering an improved fit to the observed evolution of the universe.

Now the present age of the universe is given by

$$t_0 = \int_0^\infty \frac{1}{(1+z)H(z)} dz \quad (26)$$

Using the parameter values listed in Table 1 and substituting them into Eq. (26), the present age of the Universe is found to be  $t_0 = 13.79$  Gyr. The value obtained is extremely close to the age inferred from the *Planck* 2020 observations, which estimate the age of the Universe to be 13.8 [45]. Therefore, the model parameters employed here lead to a cosmological history that is fully consistent with current high-precision measurements, reinforcing the viability of the framework in explaining the expansion age of the Universe.

To constrain the model parameters we define  $B_s = \left(\frac{B}{1+A}\right)^{\frac{1}{1+\alpha}} \frac{1}{\rho_0}$  and  $c = (1 - B_s^{1+\alpha})\rho_0^{1+\alpha}$ . Using these definitions in Eq. (9), the Hubble parameter can be written in terms of  $B_s$  as

$$H = H_0 \left\{ B_s^{1+\alpha} + (1 - B_s^{1+\alpha}) (1+z)^{3(1+A)(1+\alpha)} \right\}^{\frac{1}{2(1+\alpha)}} \quad (27)$$

The values of  $B_s$  and  $\alpha$  corresponding to the minimum  $\chi^2$  are determined from the contour plot shown in Fig. 6, for  $H_0 = 72 \text{ km s}^{-1} \text{ Mpc}^{-1}$  and  $A = 0.025$ . The corresponding parameter ranges within the  $1\sigma$  confidence region are listed in Table 2.

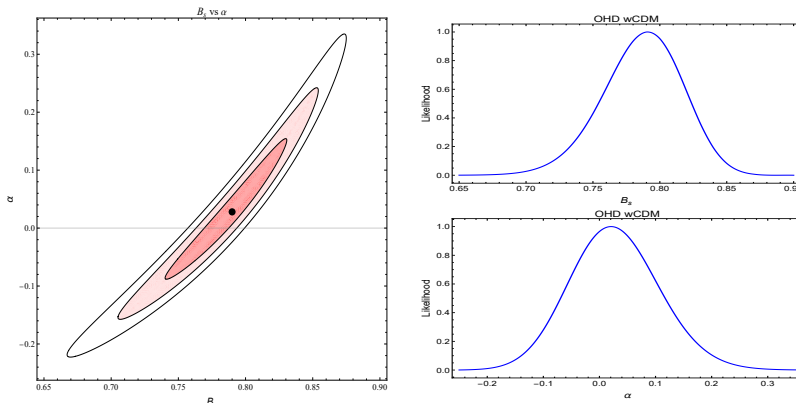


Figure 6:  $B_s$  vs  $\alpha$  graph with likelihood

Table 2: Best-fit values of the  $B_s$  and  $\alpha$  using Hubble-57 data ( $1\sigma$  confidence region).

Parameter	$H_0$ (km s $^{-1}$ Mpc $^{-1}$ )	$A$	$\chi_m^2$	$B_s$	$\alpha$
<b>Best-fit values</b>	72	0.025	46.35	0.79	0.028
<b>Range (<math>1\sigma</math> region)</b>	–	–	–	0.7401, 0.8307	–0.0882, 0.1544

It is worth noting that the earlier study by B. C. Paul et al. [46] found  $A = 0.0101$ ,  $B_s = 0.8450$  and  $\alpha = 0.3403$ , values that are marginally higher than those derived in the present analysis.

Using the parameter values in Table 2 we obtain from Eqs. (26) and (27)  $t_0 = 14.054$  Gyr. This estimate is marginally larger than the age reported by the *Planck* 2020 analysis [45], but the difference lies within current observational uncertainties. Therefore, the result supports the consistency of the Modified Chaplygin Gas model with contemporary cosmological observations.

As discussed earlier, the key Eq. (10) does not admit an explicit analytical solution in a simple functional form of time. Consequently, it is not possible to express the evolution of cosmological quantities—such as the scale factor, the flip time, and other dynamical parameters—in a closed form. To overcome this limitation and to determine the flip time along with other physical characteristics of the cosmological model, we adopt an *alternative approach* [38, 47] in the following section.

## 4 An Alternative Formulation

Since the scale factor increases with time in an expanding universe, the last term in Eq. (10) becomes negligible compared to the second term when expanded binomially. Therefore, the results obtained from a first-order approximation of the expanded Eq. (10) are particularly relevant. In what follows, we present the exact solution corresponding to this first-order approximation. Accordingly, at the late stage of cosmic evolution, the first-order approximation of Eq. (10) takes the form

$$3\frac{\dot{a}^2}{a^2} = \left(\frac{B}{1+A}\right)^{\frac{1}{1+\alpha}} + \frac{1}{1+\alpha} \left(\frac{1+A}{B}\right)^{\frac{\alpha}{1+\alpha}} \frac{c}{a^{3(1+A)(1+\alpha)}} \quad (28)$$

For economy of space we skip the intermediate steps and write the final solution as,

$$a(t) = a_0 \sinh^n \omega t \quad (29)$$

$$\text{where, } a_0 = \left\{ \frac{c(1+A)}{B(1+\alpha)} \right\}^{\frac{1}{3(1+A)(1+\alpha)}}, n = \frac{2}{3(1+A)(1+\alpha)} \text{ and } \omega = \frac{\sqrt{3}}{2} (1+A)^{\frac{1+2\alpha}{2(1+\alpha)}} (1+\alpha) B^{\frac{1}{2(1+\alpha)}}$$

The evolution of the scale factor  $a(t)$  with time  $t$  for the Modified Chaplygin Gas (MCG) model is shown in Fig. 7. While the MCG model is usually studied in its asymptotic limits, a first-order approximation reveals a continuous evolution of  $a(t)$  from an early decelerating phase to a late-time accelerated expansion, as also indicated by Eq. (29).

Using Eqs. (6), (7) and (29) we can write the expression of density and pressure as follows,

$$\rho = 3n^2 \omega^2 \coth^2 \omega t = \left(\frac{B}{1+A}\right)^{\frac{1}{1+\alpha}} \left\{ 1 + (1+z)^{\frac{2}{n}} \right\} \quad (30)$$

and

$$p = n\omega^2 \left\{ (2-3n) \coth^2 \omega t - 2 \right\} = - \left(\frac{B}{1+A}\right)^{\frac{1}{1+\alpha}} \left[ 1 - \{\alpha + A(1+\alpha)\} (1+z)^{\frac{2}{n}} \right] \quad (31)$$

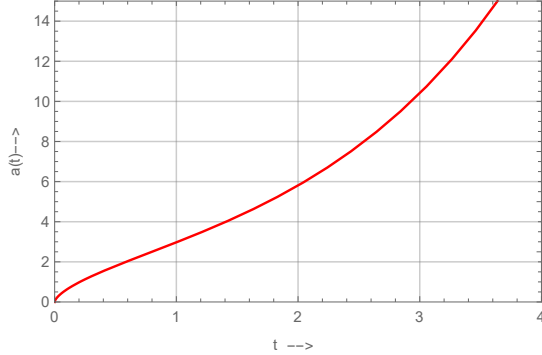


Figure 7: The variations of  $a(t)$  and  $t$ .

We now discuss the evolution of various cosmological parameters within this first-order approximation framework.

#### 4.1 Deceleration Parameter :

From Eq. (29), we obtain the expression of deceleration parameter as

$$q = -\frac{1}{H^2} \frac{\ddot{a}}{a} = \frac{1 - n \cosh^2(\omega t)}{n \cosh^2(\omega t)} = \frac{1}{n \left\{ 1 + (1+z)^{-\frac{2}{n}} \right\}} - 1. \quad (32)$$

This expression shows that the exponent  $n$  determines the nature of evolution of the deceleration parameter  $q$ . A closer inspection reveals that

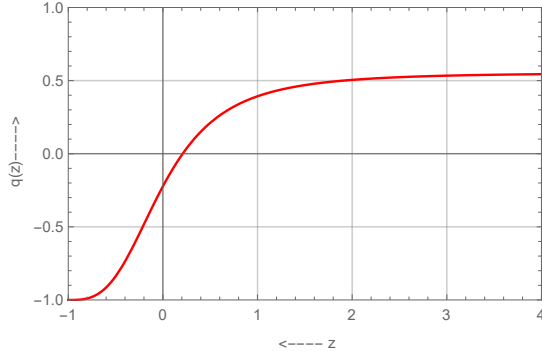


Figure 8: The variations of  $q(z)$  and  $z$ .

- (i)  $n \geq 1$  gives always acceleration, no flip occurs in this condition. But for  $n \geq 1$ ,  $\alpha < -\frac{1+3A}{3(1+A)}$  which is physically unrealistic for  $A > 0$  &  $\alpha > 0$ .
- (ii)  $0 < n < \frac{2}{3}$  gives the early deceleration and late acceleration in the conditions for  $A > 0$  &  $\alpha > 0$ , so desirable feature of *flip* occurs which agrees with the observational analysis.

At the time of flip  $q = 0$  and the flip time  $t_f$  is given by

$$t_f = \frac{1}{\omega} \cosh^{-1} \left( \frac{1}{\sqrt{n}} \right) = \frac{1}{\omega} \cosh^{-1} \sqrt{\frac{3(1+A)(1+\alpha)}{2}} \quad (33)$$

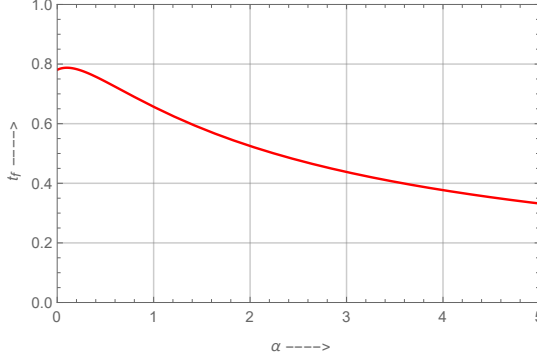


Figure 9: The variations of  $t_f$  and  $\alpha$ .

Fig. 9 shows the flip time  $t_f$  as a function of  $\alpha$ . The plot clearly indicates that smaller values of  $\alpha$  correspond to a later transition to the accelerated phase of expansion. This behavior is consistent with Eq. (2) for larger  $\alpha$ , the negative pressure associated with the fluid grows more rapidly with cosmic expansion, causing the Universe to enter the accelerating regime earlier. Therefore, the trend observed in Fig. 9 is fully consistent with the theoretical expectations derived from Eq. (2).

Now the redshift at the time of flip is

$$z_f = \left( \frac{n}{1-n} \right)^{\frac{n}{2}} - 1 \quad (34)$$

To obtain acceleration at the present epoch, the condition  $z_f > 0$  must hold, which leads to  $\alpha < \frac{1-3A}{3(1+A)}$ . This further implies that  $A < \frac{1}{3}$  in order to ensure  $\alpha > 0$ , indicating that the model parameters must lie within these bounds to produce a physically consistent universe dominated by dark energy-like behavior, characterized by negative effective pressure and accelerated expansion.

Now we discuss the evolution of deceleration parameter at different epoch as follows:

- (i) At the early epoch of the universe, i.e., during the radiation-dominated era corresponding to high redshift  $z$ , we obtain from Eq. (32)

$$q = \frac{1}{n} - 1 = \frac{3(1+A)(1+\alpha)}{2} - 1. \quad (35)$$

For  $q$  to be positive, the condition  $\alpha > -\frac{1+3A}{3(1+A)}$  must be satisfied. In particular, for any positive value of  $A$ , this implies that  $\alpha$  must also be positive.

- (ii) At the present epoch, i.e., at  $z = 0$ , Eq. (32) reduces to

$$q = \frac{1}{2n} - 1 = \frac{3(1+A)(1+\alpha)}{4} - 1. \quad (36)$$

Since the present universe is undergoing accelerated expansion, we require  $q < 0$ . This condition implies  $\alpha < \frac{4}{3(1+A)} - 1$ . Moreover, using the bound  $0 \leq A \leq \frac{1}{3}$ , we conclude that  $A < \frac{1}{3}$ .

(iii) At the late universe, the Eq. (32) gives  $q = -1$  which corresponds to  $\Lambda$ CDM model.

Fig. 8 shows the deceleration parameter  $q$  versus redshift  $z$  in the Modified Chaplygin Gas model, illustrating a smooth transition from early deceleration ( $q > 0$ ) to late-time acceleration ( $q < 0$ ) at the flip redshift  $z_f$ , without separate dark matter or dark energy components.

## 4.2 Effective equation of state:

The effective equation of state  $w_e$  is given by

$$w_e = \frac{p}{\rho} = \frac{2-3n}{n^2} - \frac{2}{3} \tanh^2 \omega t = -\frac{1 - \{\alpha + A(1 + \alpha)\}(1 + z)^{\frac{2}{n}}}{1 + (1 + z)^{\frac{2}{n}}} \quad (37)$$

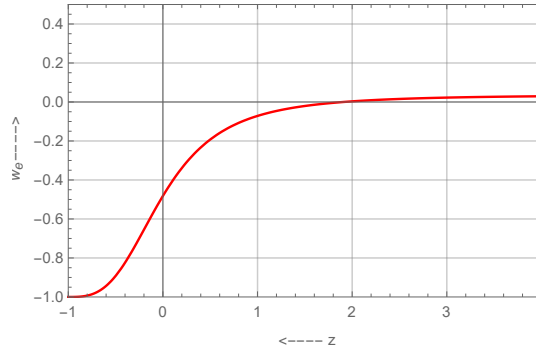


Figure 10: The variations of  $w_e$  and  $z$ .

(i) **Early Epoch:** In the high-redshift limit, the effective equation-of-state parameter can be expressed, using Eq. (37), as

$$w_e \approx \alpha + A(1 + \alpha), \quad (38)$$

which remains positive for all physically admissible values of  $A$  and  $\alpha$ . This corresponds to a decelerating, radiation-like phase of the universe.

(ii) **Dust dominated Epoch:** In the dust-dominated era, where  $w_e = 0$ , the corresponding redshift  $z_{dust}$  can be obtained from Eq. (37) as

$$z_{dust} = \left\{ \frac{1}{\alpha + A(1 + \alpha)} \right\}^{\frac{n}{2}} - 1. \quad (39)$$

This relation shows that  $z_{dust} > z_f$ , which is consistent with the expected cosmological timeline. It signifies that the transition to an accelerating phase occurs after the dust-dominated epoch—marking the evolution from matter domination to a dark energy–driven universe.

(iii) **Present Epoch:** At  $z = 0$ , Eq. (37) reduces to

$$w_e \approx -\frac{1 - \{\alpha + A(1 + \alpha)\}}{2}. \quad (40)$$

Since  $\alpha < \frac{1-3A}{3(1+A)}$  and  $A < \frac{1}{3}$ , we have  $w_e < 0$ , indicating that the present universe is undergoing an accelerated expansion.

(iv) **Late-Time Limit:** As  $z \rightarrow -1$ , Eq. (37) reduces to  $w_e \approx -1$ , showing that the model asymptotically approaches a cosmological constant-dominated phase, effectively reproducing the  $\Lambda$ CDM scenario.

Fig. 13 shows the effective equation of state  $w_e$  versus redshift  $z$  in the MCG model, illustrating a smooth transition from early deceleration ( $w_e > 0$ ) to late-time acceleration ( $w_e \rightarrow -1$ ). In summary,  $w_e$  evolves from a positive, decelerating value in the early universe, through a negative, accelerating phase at the present epoch, to a  $\Lambda$ CDM-like state at late times, providing a consistent description of cosmic evolution.

### 4.3 Observational constraint:

The Hubble parameter can now be expressed in terms of the matter density parameter  $\Omega_m$  ( $= \frac{c}{\rho_0^{1+\alpha}}$ ) using Eq. (28) as

$$H = H_0 \Omega_m^{\frac{1}{1+\alpha}} \left\{ \left( \frac{1 - \Omega_m}{\Omega_m} \right)^{\frac{1}{1+\alpha}} + \frac{1}{1+\alpha} \left( \frac{\Omega_m}{1 - \Omega_m} \right)^{\frac{\alpha}{1+\alpha}} (1+z)^{3(1+A)(1+\alpha)} \right\}^{\frac{1}{2}} \quad (41)$$

A contour plot, shown in Fig. 11, has been generated using Eq. (41). The best-fit values of the parameters  $\alpha$  and  $\Omega_m$  for  $H_0 = 71 \text{ km s}^{-1} \text{ Mpc}^{-1}$  and  $A = 0.002$ , along with their corresponding  $1\sigma$  confidence ranges, are listed in Table 3.

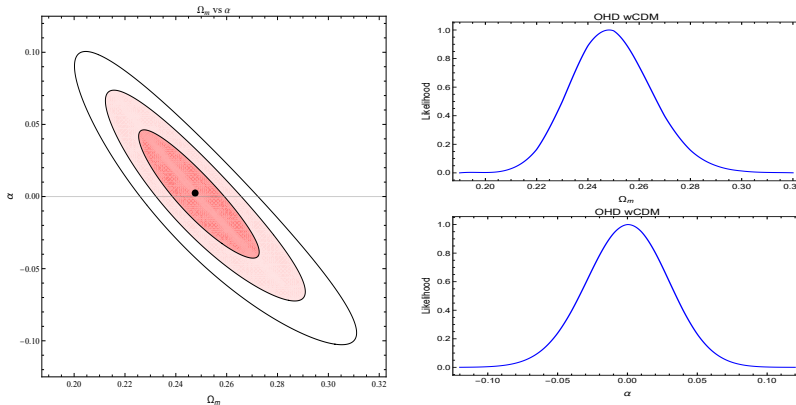


Figure 11:  $\Omega_m$  vs  $\alpha$  graph with likelihood

Table 3: Best-fit values of the  $\Omega_m$  and  $\alpha$  using Hubble-57 data ( $1\sigma$  confidence region).

Parameter	$H_0$ ( $\text{km s}^{-1} \text{ Mpc}^{-1}$ )	$A$	$\chi_m^2$	$\Omega_m$	$\alpha$
Best-fit values	71	0.002	44.87	0.248	0.0024
Range ( $1\sigma$ region)	—	—	—	0.2254, 0.2728	-0.0427, 0.0462

From Eqs. (26) and (41), and using the parameter values listed in Table 3, we obtain the present age of the universe as  $t_0 = 13.94$  Gyr. This value is slightly higher than the estimate reported by the Planck 2020 results [45]. Furthermore, to constrain the model parameters, we define  $B_s = \left( \frac{B}{1+A} \right)^{\frac{1}{1+\alpha}} \frac{1}{\rho_0}$ , which

allows the Hubble parameter to be expressed in terms of  $B_s$  as

$$H = H_0 \left\{ B_s + \frac{1}{1+\alpha} \frac{(1-B_s^{1+\alpha})}{B_s^\alpha} (1+z)^{3(1+A)(1+\alpha)} \right\}^{\frac{1}{2}} \quad (42)$$

The values of  $B_s$  and  $\alpha$  corresponding to the minimum  $\chi_m^2$  are determined from the contour plot shown in Fig. 12, for  $H_0 = 71 \text{ km s}^{-1} \text{ Mpc}^{-1}$  and  $A = 0.002$ , with the corresponding  $1\sigma$  confidence ranges presented in Table 4. It is found that  $\alpha < 1$ , in contrast to the pure Chaplygin Gas model, for which  $\alpha = 1$ .

It is worth mentioning that the condition derived in Sec. 3.2,  $B > \frac{c}{2}(1+3A)(1+A)$ , or equivalently  $\frac{B_s^{1+\alpha}}{\Omega_m} > \frac{1+3A}{2}$ , is also satisfied by the values obtained from our alternative approach, thereby confirming the consistency of the results.

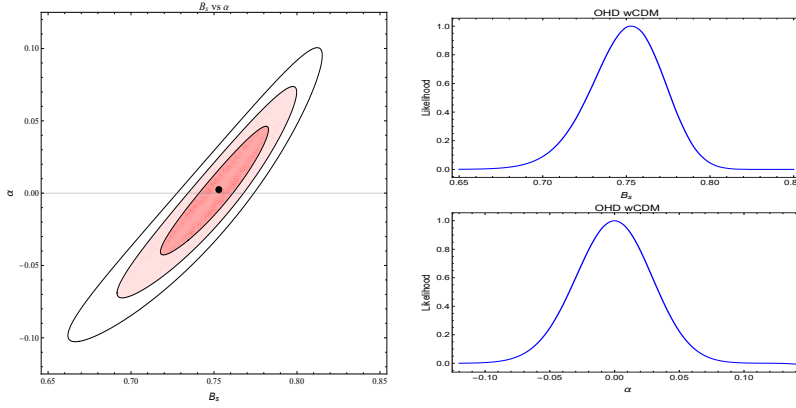


Figure 12:  $B_s$  vs  $\alpha$  graph with likelihood

Table 4: Best-fit values of the  $B_s$  and  $\alpha$  using Hubble-57 data ( $1\sigma$  confidence region).

Parameter	$H_0$ ( $\text{km s}^{-1} \text{ Mpc}^{-1}$ )	$A$	$\chi_m^2$	$B_s$	$\alpha$
Best-fit values	71	0.002	44.87	0.7527	0.0024
Range ( $1\sigma$ region)	—	—	—	0.7177, 0.7828	-0.0427, 0.0462

We also determine the present age of the universe using the parameter values from Table 4. From Eqs. (26) and (42), we calculate  $t_0 = 13.94$  Gyr. This value is slightly higher than the result obtained from Planck 2020 data [45]. This slight discrepancy may be attributed to the fact that these datasets probe different epochs and aspects of cosmic evolution. Moreover, variations in the assumed values of the Hubble constant and other cosmological parameters across different analyses naturally lead to minor differences in the estimated age of the universe.

## 5 Negative Constant ( $C < 0$ ) :

### 5.1 Phantom field

Distinctly new cosmological behaviour emerges when the arbitrary integration constant is taken as  $c < 0$ . In this case, the energy density increases with the scale factor, mimicking a phantom dark energy scenario, and eventually asymptotically approaches a constant value corresponding to a cosmological constant at late times. We get from Eq. (9) that for the matter field to be well behaved the condition

$$a^{3(1+A)(1+\alpha)} > \frac{C(1+A)}{B} \quad (43)$$

need to be satisfied. So a minimal value of the scale factor given by

$$a(t)_{min} = \left[ \frac{C(1+A)}{B} \right]^{\frac{1}{3(1+A)(1+\alpha)}} \quad (44)$$

we consider a homogeneous scalar field  $\phi(t)$  and a potential  $U(\phi)$  to describe the Lagrangian as

$$L_\phi = \frac{\dot{\phi}^2}{2} - U(\phi) \quad (45)$$

and now set the energy density of the field equal to that of the Modified Chaplygin gas as

$$\rho_\phi = \frac{\dot{\phi}^2}{2} - U(\phi) = \rho \quad (46)$$

The corresponding "pressure" coincides with the Lagrangian density as

$$p_\phi = \frac{\dot{\phi}^2}{2} - U(\phi) = p \quad (47)$$

These gives

$$\dot{\phi}^2 = \frac{c(1+A)}{\rho^\alpha a^{3(1+A)(1+\alpha)}} \quad (48)$$

When the constant  $c < 0$ , the kinetic term becomes negative, i.e.,  $\dot{\phi}^2 < 0$ . In this case, we may define a real scalar field  $\psi$  through the relation  $\phi = i\psi$ . Accordingly, the Lagrangian of the field  $\phi(t)$  can be rewritten as

$$L_\phi = \frac{\dot{\phi}^2}{2} - U(\phi) = -\frac{1}{2}\dot{\psi}^2 - U(i\psi) \quad (49)$$

The energy density and the pressure corresponding to the scalar field  $\psi$  are as following

$$\rho_\psi = \frac{\dot{\psi}^2}{2} + U(i\psi) \quad (50)$$

and

$$p_\psi = \frac{\dot{\psi}^2}{2} - U(i\psi) \quad (51)$$

therefore, the scalar field  $\psi$  is a phantom field. This implies that one can generate phantom-like equation of state from an interacting generalized Chaplygin gas dark energy model in non-flat universe.

This naturally points to a bouncing cosmology at early times. In the past Setare [48] analyzed these possibilities in a series of work. To sum up we see that the Chaplygin model interpolates between a radiation at small  $a$  and a cosmological constant at large  $a$  but this well formulated quartessence idea breaks when a negative value of the arbitrary constant is taken. Following Barrow [49] if we reformulate the dynamics with a scalar field  $\phi$  and a potential  $U$  to simulate the Chaplygin cosmology, we find that a negative value of  $c$  implies that we transform  $\phi = i\Psi$ . In this case the expressions for the energy density and pressure corresponding to the scalar field show that it represents a phantom field.

## 5.2 Emergent Universe Scenario in the Phantom Regime

We now examine an interesting cosmological feature of the Modified Chaplygin Gas (MCG) model—namely, the existence of an *emergent universe* type of solution. This scenario naturally arises when the integration constant appearing in the energy conservation relation takes a negative value  $c < 0$ , leading to a phantom-like effective field description. We shall demonstrate that, in this case, the scale factor  $a(t)$  remains finite and nonzero even in the asymptotic past, thereby avoiding the big-bang singularity. Rewriting Eq. (10) in the following form, we have

$$\frac{\dot{a}}{a} = \frac{1}{\sqrt{3}} \left[ \frac{B}{1+A} - \frac{c}{a^{3(1+\alpha)(1+A)}} \right]^{\frac{1}{2(1+\alpha)}}. \quad (52)$$

Since, in an expanding universe, the scale factor increases with time, we can apply a first-order binomial approximation to Eq. (52), which can be expressed as

$$\frac{\dot{a}}{a} = \frac{1}{\sqrt{3}} \left( \frac{B}{1+A} \right)^{\frac{1}{2(1+\alpha)}} - \frac{1}{2\sqrt{3}(1+\alpha)} \left( \frac{1+A}{B} \right)^{\frac{1+2\alpha}{2(1+\alpha)}} \frac{c}{a^{3(1+A)(1+\alpha)}}. \quad (53)$$

The general solution of the Eq. (53) is obtained as

$$a(t) = \left[ \frac{c + 2\sqrt{3}(1+\alpha) \left( \frac{B}{1+A} \right)^{\frac{1+2\alpha}{2(1+\alpha)}} d e^{\sqrt{3}(1+\alpha)(1+A) \left( \frac{B}{1+A} \right)^{\frac{1}{2(1+\alpha)}} t}}{2 \left( \frac{B}{1+A} \right) (1+\alpha)} \right]^{\frac{1}{3(1+\alpha)(1+A)}}, \quad (54)$$

where  $d$  is an integration constant. The above expression resembles the well-known emergent form

$$a(t) = (\beta + \gamma e^{mt})^N, \quad (55)$$

where  $\beta = \frac{c(1+A)}{2B(1+\alpha)}$ ,  $\gamma = \sqrt{3}d \left( \frac{B}{1+A} \right)^{-\frac{1}{2(1+\alpha)}}$ ,  $m = \sqrt{3}(1+\alpha)(1+A) \left( \frac{B}{1+A} \right)^{\frac{1}{2(1+\alpha)}}$ , and  $N = \frac{1}{3(1+\alpha)(1+A)}$ .

Eq. (54) clearly demonstrates that an emergent–universe–type solution can naturally arise within the Modified Chaplygin Gas (MCG) framework under the first-order approximation. It is worth noting that S. Mukherjee *et al.* [29] previously derived an emergent universe solution by adopting  $\alpha = -\frac{1}{2}$  in Eq. (3). In contrast, S. Dutta *et al.* [30] reported that an emergent-type solution does not arise from the conventional MCG model. The present solution, however, described by Eq. (54), represents a new class of emergent-type behavior that naturally originates from the MCG equation of state under

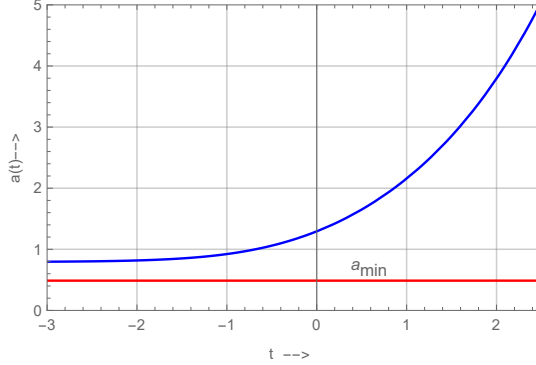


Figure 13: The variations of  $a(t)$  and  $t$ .

the first-order approximation. Interestingly, for  $c < 0$ , the model corresponds to a phantom regime, provided the physically admissible conditions  $0 < A < \frac{1}{3}$  and  $0 < \alpha < 1$  are satisfied. We now discuss the cosmological implications of this solution.

When  $c < 0$ , Eq. (52) imposes a lower bound on the scale factor to maintain a positive energy density. This condition leads directly to emergent behaviour. To ensure the positivity of the density for negative  $c$  the scale factor cannot shrink below a finite minimum value,  $a(t)_{\min}$ , as given in Eq. (44) which guarantees that the universe never reaches a singular state ( $a = 0$ ).

Taking the limit  $t \rightarrow -\infty$  in Eq. (54), the exponential term vanishes and the scale factor tends to a constant:

$$\lim_{t \rightarrow -\infty} a(t) = \left[ \frac{c(1+A)}{2B(1+\alpha)} \right]^{\frac{1}{3(1+\alpha)(1+A)}}. \quad (56)$$

which is consistent (up to normalization constants) with Eq. (44). Hence, as  $t \rightarrow -\infty$ , the universe approaches a static configuration with a finite minimum radius  $a_{\min}$ . Subsequently, it enters an exponentially expanding phase, exhibiting a de Sitter-like behavior. With further cosmic evolution, as  $t \rightarrow +\infty$ , the expansion continues to accelerate, and in the asymptotic limit, Eq. (54) reduces to  $a(t) \sim e^{Ht}$ , corresponding to the exponential expansion characteristic of the  $\Lambda$ CDM model. Thus, the model presents a smooth and singularity-free cosmological evolution, beginning from a quasi-static past and naturally evolving into a late-time accelerating universe consistent with  $\Lambda$ CDM dynamics.

For  $c < 0$ , this correspondence shows that the emergent behaviour in the MCG framework is dynamically equivalent to that of a universe dominated by a phantom scalar field, driving cosmic acceleration without an initial singularity in first approximation. The emergent universe described above is non-singular, beginning from a quasi-static state with finite  $a(t)_{\min}$  and gradually evolving into an accelerating phase dominated by dark-energy-like behaviour. The transition is smooth, and the absence of an initial singularity makes this model theoretically attractive. Therefore, within the MCG scenario, the case  $c < 0$  (phantom regime) provides a consistent and physically meaningful realization of an emergent universe.

The energy density of the universe is given by

$$\rho = \left( \frac{B}{1+A} \right)^{\frac{1}{1+\alpha}} \left( \frac{\gamma e^{mt}}{\beta + \gamma e^{mt}} \right)^2, \quad (57)$$

which remains positive during the cosmic evolution. At early times ( $t \rightarrow -\infty$ ),  $e^{mt} \rightarrow 0$ , and hence

$\rho \rightarrow 0$ , indicating a quasi-static phase with negligible energy density. As time progresses,  $e^{mt}$  increases, leading to a monotonic growth of  $\rho(t)$ . In the late-time limit ( $t \rightarrow +\infty$ ),  $e^{mt} \gg \beta$ , and the energy density approaches a constant value  $\rho \rightarrow \left(\frac{B}{1+A}\right)^{\frac{1}{1+\alpha}}$ , representing a dark energy-dominated de Sitter phase. Thus, the evolution of  $\rho(t)$  shows a smooth transition from a low-energy emergent state in the past to a constant energy density at late times, consistent with the observed accelerated expansion of the universe. The corresponding deceleration parameter  $q$  is expressed as

$$q = -1 - \frac{\beta}{N\gamma} e^{-mt}, \quad (58)$$

which remains negative throughout the cosmic evolution, indicating that the universe is always in an accelerated phase. This time-varying deceleration parameter [50] signifies that, although the universe continues to accelerate, the strength of this acceleration gradually decreases with cosmic time. Furthermore, the time derivative of  $q$  is

$$\frac{dq}{dt} = m \frac{\beta}{N\gamma} e^{-mt}, \quad (59)$$

which is positive for  $\beta, m, N, \gamma > 0$ , confirming that  $q(t)$  steadily increases with time and, as a result, the acceleration weakens as the universe evolves. Consequently,  $q(t)$  evolves from  $-\infty$  at early times ( $t \rightarrow -\infty$ ) to its asymptotic value  $q \rightarrow -1$  at late times ( $t \rightarrow \infty$ ). This behaviour characterizes a smooth transition toward a de Sitter-like accelerated phase in the far future.

The effective equation of state is given by

$$w_{\text{eff}}(t) = A - (1+A) \left(1 + \frac{\beta}{\gamma} e^{-mt}\right)^{2(1+\alpha)} \quad (60)$$

As  $t \rightarrow -\infty$ ,  $w_{\text{eff}}(t) \rightarrow -\infty$ , since the pressure term  $-\frac{B}{\rho^\alpha}$  of Eq. (3) dominates while  $\rho \rightarrow 0$ , and the universe remains quasi-static.

As  $t \rightarrow \infty$ ,  $w_{\text{eff}}(t) \approx -1$ . Therefore,  $w_{\text{eff}}(t)$  monotonically increases from  $-\infty$  toward its late-time asymptotic value. Physically, this behavior of  $w_{\text{eff}}(t)$  captures the evolution of an emergent universe scenario. At early times ( $t \rightarrow -\infty$ ),  $w_{\text{eff}} \rightarrow -\infty$  reflects the dominance of the negative pressure term, keeping the universe in a quasi-static state and avoiding an initial singularity. As time progresses,  $w_{\text{eff}}(t)$  increases monotonically, approaching a value close to  $-1$  at late times, which drives the accelerated expansion observed in the present epoch. This smooth evolution from a quasi-static past to a late-time accelerated expansion ensures a singularity-free, continuous cosmic history, consistent with the emergent universe picture.

Equation (54) demonstrates that an emergent-universe-type solution naturally arises within the Modified Chaplygin Gas (MCG) framework under the first-order approximation. While S. Mukherjee *et al.* [29] obtained such a solution for  $\alpha = -\frac{1}{2}$ , S. Dutta *et al.* [30] reported its absence in the conventional MCG model. In contrast, the present solution corresponds to a new class of emergent-type behavior arising for  $c < 0$  (phantom regime) within the physically admissible range  $0 < A < \frac{1}{3}$  and  $0 < \alpha < 1$ .

At the present epoch ( $a_0 = 1$ ), the energy density and deceleration parameter are given by

$$\rho_0 = \left(\frac{B}{1+A}\right)^{\frac{1}{1+\alpha}} (1-\beta)^2, \quad q_0 = -1 - \frac{\beta}{N(1-\beta)}, \quad (61)$$

which clearly indicates an accelerating universe. To ensure this behavior, the condition  $\beta < 1$  must be satisfied, which further implies that  $B > \frac{c(1+A)}{2(1+\alpha)}$ . The effective equation of state at the present epoch is then given by  $w_{\text{eff},0} = A - \frac{1+A}{(1-\beta)^2(1+\alpha)}$ , which becomes negative for  $0 < \beta < 1$  and  $0 < \alpha < 1$ . This result signifies that the present universe is dominated by dark energy, in agreement with observational evidence for the ongoing accelerated expansion.

In the next subsection, we perform an observational constraint analysis using the Hubble-57 dataset to determine the allowed ranges of the model parameters and to assess the viability of the emergent universe scenario within the MCG framework.

### 5.3 Observational constraint

To constrain the model parameters, we previously considered  $B_s = \left(\frac{B}{1+A}\right)^{\frac{1}{1+\alpha}} \frac{1}{\rho_0}$  and  $c = (1 - B_s^{1+\alpha})\rho_0^{1+\alpha}$ , we get the expression of Hubble parameter in terms of  $B_s$  from Eq. (53) as

$$H = H_0 B_s^{\frac{1}{2}} \left\{ 1 + \frac{1}{2(1+\alpha)} \frac{(1 - B_s^{1+\alpha})}{B_s^{1+\alpha}} (1+z)^{3(1+A)(1+\alpha)} \right\} \quad (62)$$

The values of  $B_s$  and  $\alpha$  corresponding to  $\chi_m^2$  are determined from the contour plot (see Fig. 14) and their respective ranges are given in Table 5, for  $H_0 = 80.2 \text{ km s}^{-1} \text{ Mpc}^{-1}$  and  $A = 0.003$ . We observe that  $0 < \alpha < 1$ , in contrast to the earlier work of S. Mukherjee *et al.* [29] on the emergent universe model, where the parameter was taken as  $\alpha = -\frac{1}{2}$ .

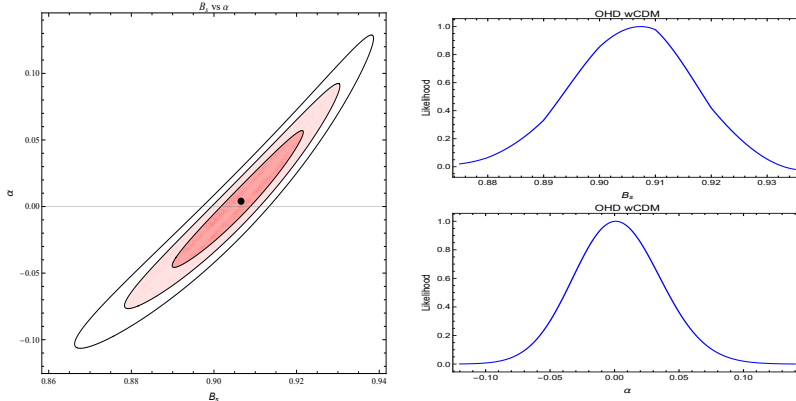


Figure 14:  $B_s$  vs  $\alpha$  graph with likelihood

Table 5: Best-fit values of the  $B_s$  and  $\alpha$  using Hubble-57 data ( $1\sigma$  confidence region).

Parameter	$H_0$ ( $\text{km s}^{-1} \text{ Mpc}^{-1}$ )	$A$	$\chi_m^2$	$B_s$	$\alpha$
Best-fit values	80.20	0.003	84.49	0.91	0.0044
Range ( $1\sigma$ region)	—	—	—	0.8899, 0.9216	-0.0457, 0.0571

It is worth mentioning that the condition derived in Sec. 5.2,  $B > \frac{c(1+A)}{2(1+\alpha)}$ , or equivalently,  $1+\alpha > \frac{1-B_s^{1+\alpha}}{B_s}$ , is also satisfied by the parameter values obtained from Eq. (62) at  $\chi_m^2$ , thereby confirming the consistency of our results.

We also determine the present age of the universe using the parameter values from Table 5. From Eqs. (26) and (62), we obtain the present age as  $t_0 = 12.92$  Gyr, which is slightly lower than the value reported by the Planck 2020 results. This comparatively lower age arises primarily due to the higher Hubble parameter ( $H_0 = 80.2$  km, s $^{-1}$ , Mpc $^{-1}$ ) and the continuous accelerated expansion associated with the  $c < 0$  emergent–universe scenario, both contributing to a faster overall expansion rate of the universe.

## 6 Raychaudhuri Equation

It may not be out of place to address and compare the situation discussed in the last section with the help of the well known Raychaudhuri equation [51], which in general holds for any cosmological solution based on Einstein’s gravitational field equations. With matter field expressed in terms of mass density and pressure Raychaudhury equation reduces to a compact form as

$$\dot{\theta} = -2(\sigma^2 - \omega^2) - \frac{1}{3}\theta^2 - \frac{8\pi G}{2}(\rho + 3p) \quad (63)$$

in a co moving reference frame. Here  $p$  is the isotropic pressure and  $\rho$  is the energy density from varied sources. Moreover other quantities are defined with the help of a unit vector  $v^\mu$  as under

$$\text{the expansion scalar } \theta = v^i_{;i} \quad (64a)$$

$$\sigma^2 = \sigma_{ij}\sigma^{ij} \quad (64b)$$

$$\text{the shear tensor } \sigma_{ij} = \frac{1}{2}(v_{i;j} + v_{j;i}) - \frac{1}{2}(\dot{v}_i v_j + \dot{v}_j v_i) - \frac{1}{3}v_{;\alpha}^\alpha(g_{ij} - v_i v_j) \quad (64c)$$

$$\text{the vorticity tensor } \omega_{ij} = \frac{1}{2}(v_{i;j} - v_{j;i}) - \frac{1}{2}(\dot{v}_i v_j - \dot{v}_j v_i) \quad (64d)$$

We can calculate an expression for effective deceleration parameter as

$$q = -\frac{\dot{H} + H^2}{H^2} = -1 - 3\frac{\dot{\theta}}{\theta^2} \quad (65)$$

In our case as we are dealing with an isotropic rotation free spacetime both the shear and vorticity scalars vanish which allows us to write,

$$\theta^2 q = 12\pi G(\rho + 3p) \quad (66)$$

Case 1: With the help of the Eqs (3), (9) and (66) we finally get,

$$\theta^2 q = 12\pi G \left[ (1 + 3A) - \frac{3(1 + A)(1 - \Omega_m)}{(1 - \Omega_m) + \Omega_m(1 + z)^{3(1+\alpha)(1+A)}} \right] \quad (67)$$

It follows from the Eq. (67) that flip occurs (i.e., at  $q = 0$ ) when

$$z_f = \left\{ \frac{2(1 - \Omega_m)}{\Omega_m(1 + 3A)} \right\}^{\frac{1}{3(1+\alpha)(1+A)}} - 1 \quad (68)$$

This is identical to Eq. (16). Moreover, setting  $A = 0$  reduces the Modified Chaplygin Gas (MCG) model to the Generalized Chaplygin Gas (GCG) model, yielding an expression identical to that obtained in our previous work [38].

**Case 2:** Now we have discussed our alternative approach in the context of Raychaudhuri equation. Now using Eqs (30), (31) and (66) we finally get after straight forward calculation that

$$\theta^2 q = 72\pi G n \omega^2 \frac{(1 - n \cosh^2 \omega t)}{\sinh^2 \omega t} = 72\pi G n \omega^2 \left[ \frac{1}{n\{1 + (1+z)^{-\frac{2}{n}}\}} - 1 \right] \quad (69)$$

We may calculate the flip time from Eq. (69) as

$$t_f = \frac{1}{\omega} \cosh^{-1} \left( \sqrt{\frac{1}{n}} \right) = \frac{1}{\omega} \cosh^{-1} \sqrt{\frac{3(1+\alpha)(1+A)}{2}} \quad (70)$$

which is identical with the Eq. (33).

Also, from Eq. (69), we can derive the expression for the redshift at flip time  $z_f$ , which is given by

$$z_f = \left( \frac{n}{1-n} \right)^{\frac{n}{2}} - 1 \quad (71)$$

The derived expression for the redshift at the flip time  $z_f$  in Eq. (71) matches perfectly with earlier findings, as shown in Eq. (34).

**Case 3:** Using Eqs (3) and (66) we get

$$\theta^2 q = \frac{3}{2} \rho \left[ 1 + 3 \left( A - \frac{B}{\rho^{\alpha+1}} \right) \right] \quad (72)$$

Since,  $\theta = 3H$  and  $\beta \ll 1$ , at present epoch ( $a_0 = 1$ ) we finally get

$$q_0 \approx -1 - \frac{1}{N} \frac{\beta}{1-\beta} \quad (73)$$

which is identical with Eq. (61).

The consistent results obtained from all approaches demonstrate the robustness of the methodology and lend further credibility to the theoretical framework adopted in this analysis.

## 7 Concluding Remarks

We explored emergent universe in general relativity with MCG for the EoS parameters:  $0 < A < \frac{1}{3}$  and  $0 < \alpha < 1$ . The cosmological model obtained here permits a universe with late-time acceleration within the framework of a spherically symmetric homogeneous model employing a modified Chaplygin gas (MCG) as the dark energy component, to accommodate the observed late acceleration of the universe. The field equation, eq. (10), is highly nonlinear and cannot be solved exactly in closed form. Previous studies addressed this by analyzing the system under extremal conditions — where the solution represents a radiation dominated universe at the early times which however asymptotically approaches the  $\Lambda$ CDM model for large values of the scale factor  $a(t)$ . However, the approach does not allow for an explicit prediction of the time evolution of the scale factor or the flip time marking the onset of acceleration because of nonlinearity. To overcome the limitations, we adopt an approximation

methodology by expanding the right-hand side of eq. (10) using a binomial series and retaining only the leading-order terms. This approximation is justified as the scale factor increases accommodating an expanding universe. Consequently, the truncated equation, presented in eq. (28), admits an exact analytical solution for the scale factor, which is given in eq. (29).

On the other hand, for  $c < 0$  it leads to a phantom-like effective field description. In this case the solution indicates that an emergent-universe solution arises naturally from the Modified Chaplygin Gas (MCG) framework with the first-order approximation. The main features are summarized below.

The generalization of the generalized Chaplygin gas model (GCG) which is MCG introduces an additional parameter  $A$ , the estimated constrained lies within the range  $0 < \alpha < \frac{1}{3}$  and  $0 < A < \frac{1}{3}$  in order to ensure that the speed of sound remains subluminal, preserving causality. Accordingly, our analysis in the paper is carried out within these admissible parameter bounds. Furthermore, cosmological observations indicate that both  $\alpha$  and  $A$  should take small values in the late universe to achieve an optimal fit with empirical data. Instead of cosmic time we have rewritten the field equation with redshift parameter  $z$ . The decelerating universe ( $z_f > 0$ ) transits to an accelerating universe when ( $z_f \rightarrow 0$ ) with the following observational constraints: (i)  $B > \frac{c}{2}(1+A)(1+3A)$  and (ii)  $\Omega_m > \frac{2}{3(1+A)}$ .

We draw the best-fit curve of the redshift  $z$  versus the Hubble parameter  $H(z)$  in Fig. 4(a), which is obtained using the Hubble 57 data set. Additionally, Fig. 4(b) compares this best-fit curve with the theoretical prediction derived from Eq. (23). The excellent agreement between these two curves across the entire range of cosmic evolution demonstrates the consistency of our model with the observational data. Furthermore, we analyze the behavior of the deceleration parameter and its flip time, the effective equation of state and other key cosmological quantities as functions of redshift  $z$ .

In Sec-4, we introduce an alternative formulation where we get the exact solution. For this reason, we can explain the evolution of the scale factor  $a(t)$ . Also calculate the flip. To get an acceleration at present epoch  $z_f > 0$  which yields  $\alpha < \frac{1-3A}{3(1+A)}$ . We have studied the deceleration parameter and effective equation of state where we note that the universe initially determined by the parameter  $A$  which however finally permits  $\Lambda$ CDM.

It is interesting to note that for  $c < 0$ , the first-order approximation yields an emergent universe with the scale factor. In this case, the universe begins with a finite, nonzero scale factor ( $a_{\min}$ ) and subsequently evolves exponentially, exhibiting a de Sitter-like expansion. This smooth transition from a quasi-static past to an accelerated future provides a singularity-free description of the early universe. As  $t \rightarrow \infty$ , the scale factor grows exponentially, consistent with the  $\Lambda$ CDM behavior within the MCG framework.

It is worth noting that Mukherjee *et al.* [29] previously obtained an emergent-universe solution by considering  $\alpha = -\frac{1}{2}$ , whereas Dutta *et al.* [30] reported that an emergent-type solution does not arise from the conventional MCG model. In contrast, we note that the cosmological solution, described by Eq. (54), permits a new class of emergent-type behavior that naturally originates from the MCG equation of state under the first-order approximation for  $c < 0$ , corresponding to the phantom regime, provided the physically admissible conditions  $0 < A < \frac{1}{3}$  and  $0 < \alpha < 1$  are satisfied.

Furthermore, the present-epoch analysis yields expressions for the model parameters. In this framework, we have adopted the condition  $\beta < 1$ , or equivalently,  $B > \frac{c(1+A)}{2(1+\alpha)}$ , to ensure physical admissibility and avoid unphysical regimes. This inequality is satisfied by the parameter values obtained from the Hubble 57 dataset, thereby confirming the physical viability of the model.

Subsequently, the entire analysis has been reinterpreted within the framework of the Raychaudhuri equation. As expected, the results are broadly consistent with previous studies, thereby reinforcing

Table 6: Best-fit parameter values obtained from Hubble-57 data for different formulation of the Modified Chaplygin Gas (MCG) model.

Model/Approach	$\chi_m^2$	$H_0$ (km s $^{-1}$ Mpc $^{-1}$ )	$A$	$\Omega_m$	$B_s$	$\alpha$	Age (Gyr)
MCG	46.48	72	0.034	0.216	-	0.0026	13.79
	44.35	72	0.025	-	0.790	0.0280	14.054
Alternative formulation	44.87	71	0.002	0.248	-	0.0024	13.94
	44.87	71	0.002	-	0.7527	0.0024	13.94
Emergent Type Solution	84.49	80.20	0.003	-	0.910	0.0044	12.92

the validity of the adopted approximation and approach. It is worth noting that although the Modified Chaplygin Gas (MCG) model has been extensively investigated over the past two decades, most analyses have primarily focused on its asymptotic or limiting cases. In contrast, the present study provides an exact analytical form of the scale factor within the proposed approximation, enabling a detailed examination of the universe's expansion history, including an explicit determination of the flip time of expansion. Moreover, the small values of  $\alpha$  obtained from both the Hubble 57 dataset and the alternative method further strengthen the model's credibility in accurately describing the dynamics of late-time cosmic acceleration satisfactorily. Furthermore, the consistency observed across all the approaches reinforces the robustness of the methodology and supports the validity of the underlying theoretical framework. Overall, the results affirm that the MCG scenario offers a theoretically sound and observationally consistent explanation for the present cosmic acceleration, without invoking additional exotic fields or modifications to general relativity.

**Declaration of competing interest** The authors declare that they have no conflict of interest.

## References

- [1] Reiss et al, *Astron. J.* **116**, 1009 (1998), arXiv: 9805201[astro-ph].
- [2] D. N. Spergel et al, *Astrophys. J. Suppl.* **148**, 175 (2003).
- [3] M. Sami and T. Padmanabhan, *Phys. Rev.* **D67**, 083509 (2003), arXiv: 0212317[hep-th].
- [4] R. R. Caldwell, *Phys. Lett.* **B 545**, 23 (2002), [ astroph/9908168].
- [5] M. Li, *Phys. Lett.* **B 603**, 1 (2004), [hep-th/0403127].
- [6] L. McAllister and E. Silverstein, *Gen. Rel. Grav.* **40**, 565 (2008), arXiv: 0710.2951.
- [7] E. Elizalde, S. Nojiri and S. Odintsov, *Phy. Rev. D* **70**, 043539 (2004).
- [8] A. Shafieloo, V. Sahni, and A.A. Starobinsky, *Phys. Rev.* **D 80**, 101301 (2009), arXiv:0903.5141.
- [9] Andrzej Krasiński, Charles Hellaby, Krzysztof Bolejko and Marie-Nöelle Célérier, *Gen. Rel. Grav.* **42**, 2453 (2010), arXiv: 0903.4070v2.
- [10] K. Bamba, S. Capozziello, S. Nojiri, and S. D. Odintsov, *Astrophys. Space Sci.* **342**, 155 (2012), arXiv: 1205.3421.

- [11] E. J. Copeland, M. Sami, and S. Tsujikawa, *Int. J. Mod. Phys. D* **15**, 1753 (2006), hep-th/0603057.
- [12] D. Panigrahi and S. Chatterjee, *Int. J. Mod. Phys. A* **21**, 6491 (2006), gr-qc/0604079.
- [13] Isha Pahwa, Debajyoti Choudhury, and T. R. Seshadri, arXiv: 1104.1925.
- [14] D. Panigrahi and S. Chatterjee, *Grav. Cosmol.* **17**, 18 (2011), arXiv:1006.0476.
- [15] S.Chatterjee and D.Panigrahi, DSU335 (AIP), 1115 (2009), arXiv: 0906.3847.
- [16] A. Y. Kamenshchik, U. Moschella, and V. Pasquier, *Phys. Lett. B* **511**, 265 (2001).
- [17] H. Sandvik, M. Tegmark, M. Zaldarriaga, and I. Waga, *Phys. Rev. D* **69**, 123524 (2004).
- [18] M. C. Bento, O. Bertolami and A. A. Sen, *Phys. Rev. D* **66**, 043507(2002).
- [19] L. Amendola, F. Finelli, C. Burigana and D. Caruran , *JCAP* **0307**, 005(2003).
- [20] H. B. Benaoum ( 2002), arXiv: 0205140 [hep-th].
- [21] U. Debnath, A. Banerjee and S. Chakraborty, *Class. Quant. Grav.* **21**, 5609 (2004), arXiv: 0411015 [gr-qc].
- [22] Y. Wu, S. Li, J. Lu and X. Yang, *Mod. Phys. Lett. A* **22**, 783(2007).
- [23] M.L. Bedran, V. Soares and M.E. Araujo, *Phys. Lett.B* **659**, 462 (2008).
- [24] S. Costa, M. Ujevic and A. F. dos Santos, *Gen. Rel. Grav.* **40**, 1683 (2008).
- [25] J. C. Fabris, H. E. S. Velten, C. Ogouyandjou and J. Tossa, 2011 *Phys. Lett B* **694**, 289(2011), arXiv: 1007.1011v1. [astro- ph.CO].
- [26] G. F. R. Ellis and R. Maartens, *Class. Quantum Grav* **21**, 223 (2004), gr-qc/0211082. (2003).
- [27] G. F. R. Ellis, J. Murugan and C. G. Tsagas, *Class. Quantum Grav* **21**, 233 (2004), gr-qc/0307112.
- [28] S. Mukherjee, B. C. Paul, S. D. Maharaj and A. Beesham, Emergent Universe in Starobinsky model(2005), gr-qc/0505103.
- [29] S. Mukherjee, B. C. Paul, N. K. Dadhich, S. D. Maharaj and A. Beesham, *Class. Quant. Grav.* **23**, 6927 (2006), arXiv:gr-qc/0605134.
- [30] Sourav Dutta, Sudeshna Mukerji, and Subenoy Chakraborty, Advances in High Energy Physics Volume (2016), Article ID 7404218; arXiv:1601.02504.
- [31] Xue-Mei Deng, *Braz. J. of Physics* **41**, 333 (2011), arXiv: 1110.1913v1 [gr-qc].
- [32] C. E. M. Batista, J. C. Fabris and M. Morita, *Gen. Rel. and Grav.* **42**,839 (2010), arXiv: 0904.3948v1[gr-qc].
- [33] J. C. Fabris, S. V. B. Goncalves and P. E. de Souza (2002), arXiv: 0207430 [astro-ph]

[34] R. Colistete Jr., J. C. Fabris, S. V. B. Goncalves and P. E. de Souza, *Int. J. Mod. Phys. D***13**, 669 (2004), arXiv: 0303338 [astro-ph].

[35] Lu et al, *Physics Lett B* **662**, 87 (2008), arxiv: 1004.3364 [astro-ph].

[36] Perlmutter S. et al, *Astrophys. J.* **517**, 565 (1999), arxiv:astro-ph/9812133.

[37] Reiss et al, *Astrophys. J.* **607**, 665 (2004).

[38] D Panigrahi, *Physics of the Dark Universe* **49**, 101982 (2025).

[39] G. Sethi, S. K. Singh and P. Kumar, *Int. J. Mod. Phys. D***15** 1089 (2006).

[40] Varun Sahni and Yuri Shtanov, ‘Cosmic Acceleration and Extra Dimensions’(2008), arXiv:0811.3839v1 [astro-ph].

[41] L. Xu, Y. Wang, H. Noh, *Eur. Phys. J. C* **72**, 1931 (2012).

[42] Hang Li, Weiqiang Yang and Liping Gai1, *Astronomy and Astrophysics* **623**, A23 (2019).

[43] J. Lu, L. Xu, J. Li, B. Chang, Y. Gui, H. Liu, *Phys. Lett. B* **662**, 87 (2008).

[44] J. A. S. Lima, J. V. Cunha and J. S. Alcaniz, *Astropart. Phys* **30**,196 (2008), arXiv: 0608469 v1 [astro-ph].

[45] E. Rosenberg, S. Gratton, G. Efstathiou, *Mon. Not. Roy. Astron. Soc.* **517**, 4620(2022), arxiv: 1204.3674.

[46] Bikash Chandra Paul, Prasenjit Thakur, Aroonkumar Beesham, *Astrophys. Space Sci.*, **361**, 336 (2016).

[47] D Panigrahi, *J. Phys.: Conf. Ser.* **1251** 0120399 (2019).

[48] M. R. Setare, *Eur. Phys. J. C***52**, 689 (2007), arXiv: 0711.0524 [gr-qc].

[49] J. D. Barrow, *Nucl. Phys. B* **310**, 743 (1988).

[50] Vijay Singh and Aroonkumar Beesham, *Int. J. of Geo. Methods in Mod. Phys.* **15**, 1850145 (2018).

[51] A. K. Raychaudhuri, *Phys. Rev.* **98**, 1123 (1955).